2016

Functional Droplets that Recognize, Collect, and Transport Debris on Surfaces

Ying Bai
University of Massachusetts Amherst

Chia-Chih Chang
University of Massachusetts Amherst

Umesh Choudhary
University of Massachusetts Amherst

Irem Bolukbasi
University of Massachusetts Amherst

Alfred J. Crosby
University of Massachusetts Amherst

See next page for additional authors

NANOMATERIALS

Functional droplets that recognize, collect, and transport debris on surfaces

Ying Bai, Chia-Chih Chang, Umesh Choudhary, Irem Bolukbasi, Alfred J. Crosby, Todd Emrick*

We describe polymer-stabilized droplets capable of recognizing and picking up nanoparticles from substrates in experiments designed for transporting hydroxyapatite nanoparticles that represent the principal elemental composition of bone. Our experiments, which are inspired by cells that carry out materials transport in vivo, used oil-in-water droplets that traverse a nanoparticle-coated substrate driven by an imposed fluid flow. Nanoparticle capture is realized by interaction of the particles with chemical functionality embedded within the polymeric stabilizing layer on the droplets. Nanoparticle uptake efficiency is controlled by solution conditions and the extent of functionality available for contact with the nanoparticles. Moreover, in an elementary demonstration of nanoparticle transportation, particles retrieved initially from the substrate were later deposited "downstream," illustrating a pickup and drop-off technique that represents a first step toward mimicking point-to-point transportation events conducted in living systems.

INTRODUCTION

Encapsulation, recognition, and transport events are central to biology and evident in the multiple types of cellular processes and mechanisms that control cell function and facilitate intracellular action (*1*–*7*). Designing materials that mimic the complex function of biology holds promise for translating the efficiency and specificity of cellular processes into simple, smart synthetic systems. This may involve, for example, integration of biologically active oligopeptides into polymers, such as the Arg-Gly-Asp tripeptide sequence. This key component of the extracellular protein fibronectin is now widely implemented in synthetic biomaterials for promoting cell adhesion or improving cell uptake (*8*). For drug delivery vehicles, integration of nuclear localization sequences into the delivery system offers the potential to realize nature's specificity in comparatively simple synthetic polymers, gels, and the like (*9*, *10*). More generally, once the fundamental characteristics of any of a variety of biological functions are identified, methods can be designed for reducing biological complexity to scalable materials, minimizing the extent of functionality required to achieve a desired outcome.

Our work is inspired by cells that function in engulfment and repair/restoration events. In one example, macrophages that engulf cellular debris take cues from surface-bound proteins that distinguish healthy cells from microbes and cancer cells (*11*). In another example, osteoclasts function in bone digestion, maintenance, and repair, working in conjunction with osteoblasts, which are crucial for bone generation (*12*, *13*). These processes represent nature's examples of encapsulation, recognition, construction, and repair that would be valuable for integration into synthetic materials but are far too complex for straightforward replication. Fortunately, Balazs and coworkers (*14*) have assessed these processes theoretically, showing, for example, that lipid vesicles in an imposed flow can recognize, pick up, and even drop off particulate materials. Our attempts to adapt these biologically inspired theoretical advances to experimental practice have focused on polymer-stabilized emulsion droplets that either (i) pick up nanoparticles (NPs) from substrates (that is, by integration of the NPs into the fluid-fluid interface with the polymer or by NP engulfment into the droplet interior phase) (*15*) or (ii) deposit encapsulated NPs into damaged regions of substrates (*16*, *17*). NP pickup using emulsion droplets was first demonstrated experimentally by Kosif *et al.* (*15*) using simple amine-functionalized NPs and droplets stabilized by polymers with activated esters that underwent amidation with the amine-rich NPs. NP pickup performed in this fashion can be viewed as mimicking the action of osteoclasts, and it provides a springboard for examining the concept in materials systems with compositions mirroring those of biology. Notably, other complex cellular functions such as endocytosis (*2*) and intracellular trafficking (*18*) can be modeled using NPs with materials systems that mimic cellular compartmentalization and allow for internalization and selective placement of NPs. Polymersomes (that is, vesicles composed of amphiphilic block copolymers) can mimic cellular processes using adhesive ligands that bind to substrates that display inflammatory markers (*19*). Similarly, Jin *et al.* (*20*) described a synthetic variant of cell aggregation using polymersomes that have complementary functionality and enable light-induced reversible assembly and disassembly.

This work addresses materials systems that adapt the concepts described above to hydroxyapatite (HA) NPs, which have a calcium phosphate–rich structure [$Ca_5(OH)(PO_4)_3$] that reflects the principal materials composition of bone. This is an especially suitable test case for examining "osteodroplets" as vehicles for the collection, transport, and deposition of debris (*21*–*28*). Because HA NPs are insoluble in organic solvents and show no affinity for stabilizing oil-water interfaces, we speculated that the presence of coordinating functionality within polymer-stabilized emulsion droplets would be required for their recognition and pickup. Thus, a catechol-containing polymer surfactant was designed to promote electrostatic interactions with HA NPs (*29*–*31*) for their retrieval, as illustrated schematically in Fig. 1. The process was visualized by fluorescence microscopy with dye-labeled NPs to track their location during the course of the experiments, and it confirmed that the presence of adhesion-promoting catechol functionality on the droplets was crucial for successful implementation of the concept.

RESULTS AND DISCUSSION

Synthesis of catechol-functionalized polymer surfactants

The emulsion droplets used in our experiments were stabilized by amphiphilic polyolefins consisting of a hydrophobic poly(cyclooctene) backbone and pendent phosphorylcholine (PC) groups that were prepared by ring-opening metathesis polymerization (ROMP), as

Polymer Science and Engineering Department, University of Massachusetts, 120 Governors Drive, Amherst, MA 01003, USA.
*Corresponding author. Email: tsemrick@mail.pse.umass.edu

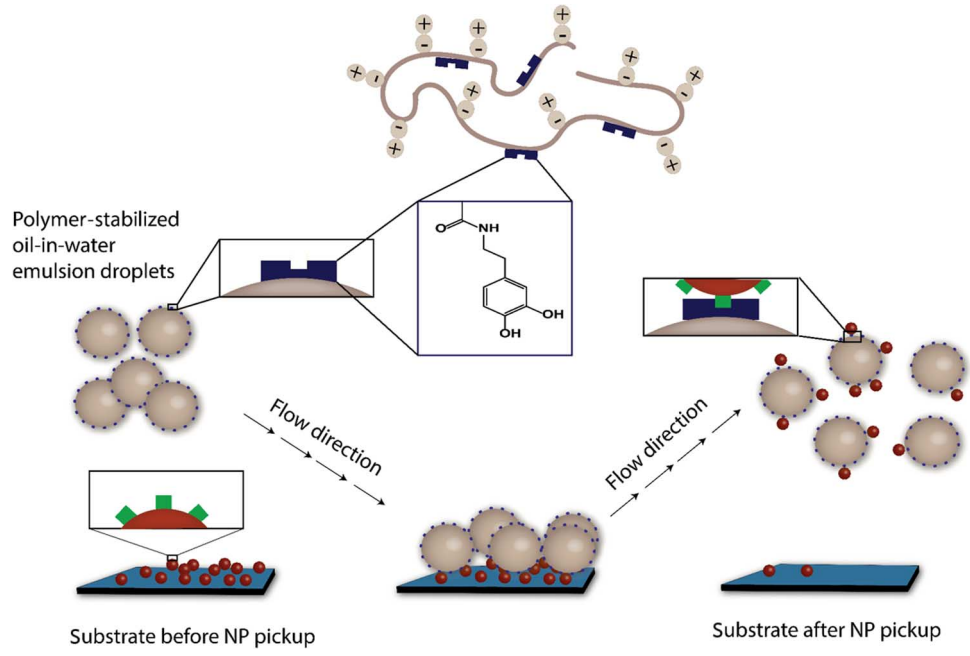

Fig. 1. Illustration of HA NP capture using functional, polymer-stabilized emulsion droplets.

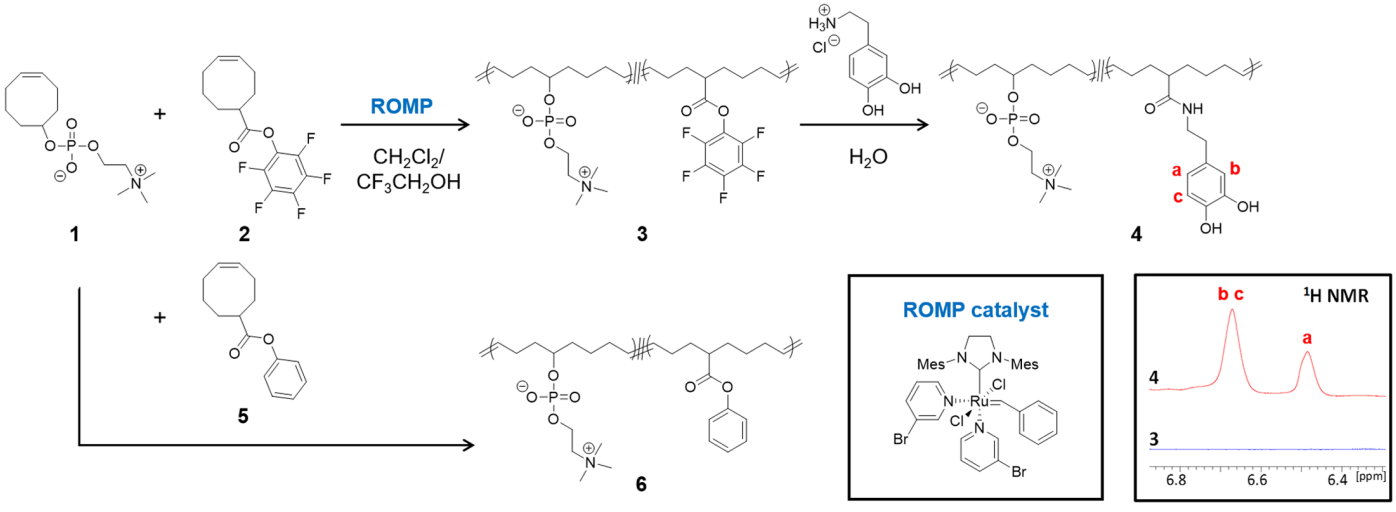

Fig. 2. Synthesis of polymers 3, 4, and 6. (Insets) Chemical structure of the 3-bromopyridine–substituted Grubbs catalyst and the aromatic region of the ^{1}H NMR spectra of polymers **3** and **4**.

shown in Fig. 2. The PC groups were selected with the intention of imparting nonfouling properties to the droplets and preventing their irreversible adsorption on substrates (*32*). In catechol-containing PC-polyolefin **4**, catechols were chosen for their known affinity for calcium (*33*) and potential to adhere to HA NPs. Adaptation of catechols to synthetic systems is inspired by their role in underwater adhesion in mussel foot proteins, which has been exploited in polymeric adhesives for tissues, bones, and teeth. Chirdon *et al.* (*34*) noted the work of adhesion of catechols on HA surfaces to be ~88 mJ/m^2, which is greater than that observed for short alkyl chain carboxylates, amines, and alcohols. Thus, we anticipated these "PC-catechol" polymers to be potentially effective in contributing a blend of nonfouling (PC) and adhesion-promoting (catechol) functionality into one synthetic surfactant system.

Because catechol groups are prone to interfering with olefin metathesis chemistry (*35*), we chose to prepare reactive polymer precursors that allow facile postpolymerization inclusion of catechols via dopamine. As shown in Fig. 2, pentafluorophenyl ester (PFPE)–containing cyclooctene **2** was copolymerized with PC-substituted cyclooctene **1** to afford polymer **3**, which has PFPE groups pendent to the backbone. Amidation of polymer **3** with 3 eq of dopamine hydrochloride relative to PFPE in water yielded polymer **4**, which was purified by dialysis against methanol and water, followed by lyophilization. Fourier transform infrared spectroscopy showed that the PFPE carbonyl stretch

at 1782 cm^{-1} disappeared, and a new amide carbonyl stretch at 1641 cm^{-1} confirmed successful amidation. ^{13}C nuclear magnetic resonance (NMR) spectroscopy (fig. S1) showed a shift in the carbonyl resonance from 173.3 to 178.4 ppm, suggesting quantitative ester-to-amide conversion. ^{1}H NMR spectroscopy (fig. S2) confirmed the integrity of the catechol functionality from the characteristic resonances at 6.67 and 6.48 ppm. By integrating the CH_2 proton signal adjacent to the catechol groups at 2.60 ppm against the polymer backbone olefin signals at 5.37 ppm, catechol incorporation in polymer **4** was estimated to be 23 and 40 mole percent (mol %) for the samples used in these studies. Unlike conventional surfactants, these PC-catechol polymers are materials with relatively high molecular weights, estimated by gel permeation chromatography (GPC) to be in the 70-kDa range. The presence of catechols along the PC-polyolefin backbone did not interrupt the surfactant properties of PC-polyolefins: polymer **4** was found to effectively stabilize oil-in-water droplets, with pendant drop tensiometry measurements yielding interfacial tension values of ~12.5 mN/m at the tricholorobenzene (TCB)/water interface (fig. S3C). This surfactant character assured the suitability of these polymers for stabilizing oil-in-water emulsions and testing the NP pickup concept. For control experiments, PC-polyolefin **6**, containing 25 mol % of phenyl ester groups in place of the catechols (Fig. 2), was synthesized by ROMP of PC-substituted cyclooctene **1** and phenyl ester–containing cyclooctene **5** (*15*), rationalizing that such a structure would display interfacial properties on order of polymer **4** but without the functionality needed for electrostatic interactions with HA NPs. Polymer **6** was found to exhibit comparable interfacial tension values of ~8.0 mN/m, confirming its capability to stabilize oil-in-water droplets (fig. S3C).

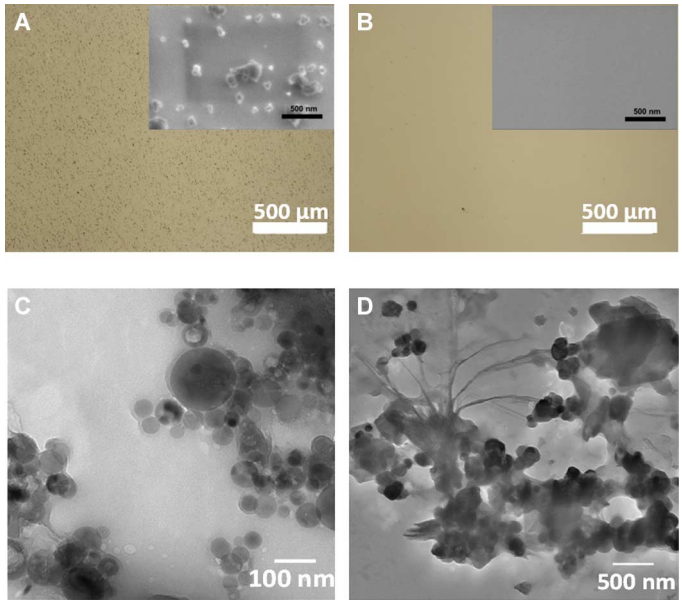

Fig. 3. Optical micrographs and TEM images of HA NPs before and after pickup. (**A**) Optical micrograph (scale bar, 500 µm) of HA NPs coated on a Si substrate before attempted NP pickup (inset: corresponding SEM image of the same substrate as the outset; scale bar, 500 nm). (**B**) Optical (main) and SEM (inset) images of the Si substrate after NP pickup (scale bars, 500 µm for the outset and 500 nm for the inset). (**C**) TEM image of dried HA NPs (scale bar, 100 nm). (**D**) TEM image of a portion of a dried droplet showing the presence of HA NPs (scale bar, 500 nm).

HA NP pickup

Polymer-stabilized oil-in-water emulsion droplets were generated by shaking an aqueous solution of polymer **4** or polymer **6** (2.0 mg/ml) in an organic solvent (for example, TCB, chloroform, or toluene) [20:1 water/oil (v:v)]. This simple preparation afforded droplets of 100 to 300 µm in diameter (fig. S3). NP pickup experiments were performed with TCB as the organic solvent, which benefits from its low miscibility with water (~50 mg/liter) and high density (1.46 g/ml) that promotes droplet contact with the substrate. An aqueous suspension of HA NPs (purchased from Sigma-Aldrich) was subjected to centrifugation, and the residue obtained was redispersed as a solution (~4.0 mg/ml) in ethanol that is stable for several hours and useful for casting onto substrates. These suspensions were applied by spin coating onto rectangular substrates (2 cm^2) of various compositions, including silicon, poly(dimethylsiloxane) (PDMS), mica, poly(ethylene terephthalate) (PET), and poly(ether ether ketone) (PEEK). A custom flow cell fabricated for our experiments consisted of a Teflon block (7.5-cm length × 5.0-cm width × 2.0-cm depth), with an embedded well (3.0 cm × 1.0 cm × 0.5 cm) into which the substrate was placed (see fig. S4 for schematic and image). Emulsion droplets were generated by mixing an aqueous solution of polymer (10 ml, 2 mg/ml) with TCB (0.5 ml) and pumping the droplets through the system over the HA NP–coated substrate under laminar flow (flow rate, 0.5 ml/s; Reynolds number, ~300) in pulsed intervals of 5 s of flow and 30 s of rest. Optical, fluorescence, and electron microscopy images of the substrates and droplets were recorded before and after the experiments.

Figure 3A shows an optical microscopy image (magnification, ×5) of a Si substrate at the outset of an experiment, where NP aggregation produces a contrast on the surface, readily visible by optical microscopy; the inset shows that scanning electron microscopy (SEM) reveals NPs in small and large clusters on the substrate. Oil-in-water emulsion droplets were prepared by shaking 10 ml of an aqueous (pH 7) solution of polymer **4** (2 mg/ml) with 0.5 ml of TCB. The polymer-stabilized droplets traversed the substrate over 150 pulsed intervals, after which the substrates were examined again. As seen in Fig. 3B, the original optical contrast on the substrate is absent, suggesting effective removal of NP debris by the droplets. SEM imaging (Fig. 3B, inset) of numerous regions of the substrate revealed a complete absence of NPs. Transmission electron microscopy (TEM) analysis (Fig. 3C) was additionally useful; the original HA NPs on carbon-coated copper grids were seen as polydisperse and roughly spherical structures with diameters of approximately 30 to 300 nm. TEM images of dried emulsion droplets after pickup (Fig. 3D) showed NPs similar to those of the commercial sample, along with some amorphous features attributed to polymer surfactant.

Control experiments confirmed the crucial role of chemical functionality in the polymer-stabilized droplets for NP pickup. When the pulsed flow was conducted with water (pH 7) only (that is, without droplets), little to no loss of NPs from the substrate was observed (fig. S5, A and B). In addition, no significant decrease in NP density on the substrate (observed by optical microscopy and SEM) was seen when the pulsed flow was conducted with oil-in-water droplets stabilized by polymer **6**, which lacks catechol functionality (fig. S5, C and D). This observation that "smart droplets," which have suitable functionality for interaction with the selected NPs, are required for NP pickup holds promise for designing selective systems that may recognize and transport any of a range of NP compositions.

Pickup efficiency

We attempted to evaluate the efficiency of HA NP pickup using ImageJ analysis on the optical micrographs, converting intensity threshold into

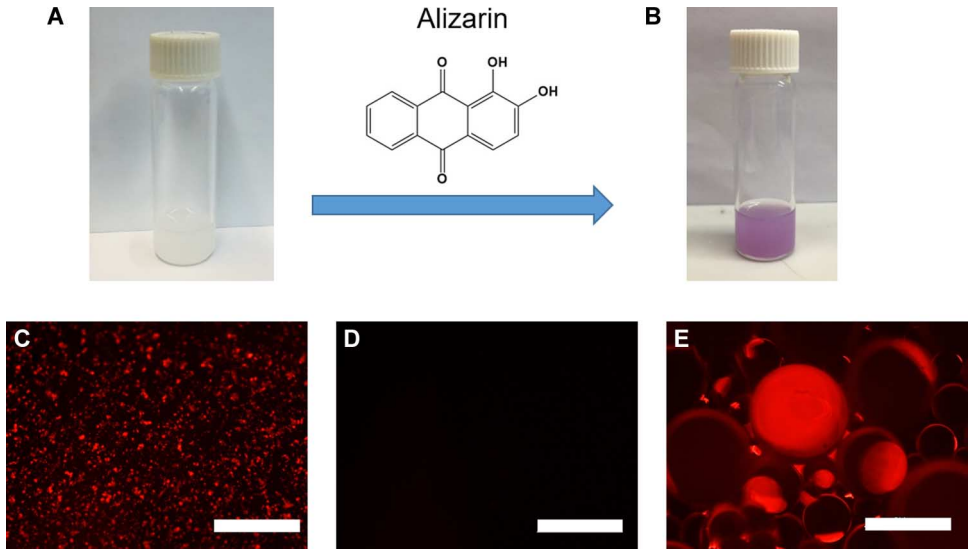

Fig. 4. Visualization of HA NP pickup using alizarin-labeled NPs. (**A**) Commercial HA NP suspended in ethanol before staining. (**B**) Alizarin-labeled HA NPs suspended in ethanol. (**C**) Fluorescence micrograph of alizarin-labeled HA NP–coated substrate. (**D**) Same substrate after HA NP pickup using polymer **4**–stabilized droplets. (**E**) Fluorescence micrograph of polymer **4**–stabilized droplets following NP pickup. Scale bars (C to E), 500 μm.

area of coverage, and defining efficiency as the relative reduction in dark regions following NP pickup, as expressed in Eq. 1

$$\eta = (1 - A_1/A_0) \times 100\% \quad (1)$$

where η denotes pickup efficiency, and A_0 and A_1 represent the dark areas before and after NP pickup, respectively. Analyses were conducted on at least five different regions of three identically treated samples. As seen in Fig. 3, the extent of NP debris on the substrate decreased by more than 99%, suggesting an effective and efficient experimental design. In contrast, ImageJ analysis of substrates used in control experiments that involved water only (no droplets) (fig. S5, A and B) showed that nearly 100% of the NPs remained on the substrate. NP pickup was similarly ineffective when using droplets stabilized by polymer **6**, showing only ~5% NP reduction (fig. S5, C and D).

We also studied several control factors by tuning the polymer surfactant and aqueous phase environment, which potentially influence pickup efficiency, such as the extent of catechol functionality on the polymer, pH, and the presence of ions in solution. Although polymer **4**, having 23 and 40 mol % of catechol-containing monomers, exhibited efficient NP pickup in Milli-Q water (pH ≈ 7), the efficiency decreased to about 70% under basic conditions (0.1 M NaOH solution; fig. S6). Because basic conditions can accelerate catechol oxidation (*36*), these conditions may be expected to reduce the droplet affinity for the HA NPs. Using ^{1}H NMR, we find that the catechol functionality of 0.1 M NaOH solution in D_2O remained intact, as evidenced by the resonances at 6.57 and 6.29 ppm even after the solution was exposed to air for 2 hours. We also noted that the change in pickup efficiency was minimal in 0.1 M NaOH solution, and complete NP removal from the Si substrate was found by dissolving polymer **4** with 40 and 23 mol % of catechols in pH 7 water. To better understand the influence of pH in the aqueous polymer solution, we attempted NP pickup using droplets prepared from polymer **4** under acidic conditions (that is, pH 4 HCl). However, rinsing the HA NP–coated substrate with pH 4 water, without any droplets, led to removal of the NPs, presumably due to their dissolution in acidic water (fig. S7, A and B).

Pickup experiments were also performed in salt water, specifically to evaluate the effect of calcium ions on the outcome of the experiments. Polymer **4** with 40 mol % of catechol was dissolved in 1 and 10 mM $CaCl_2$ solution, respectively, and used in NP pickup experiments with 150 intervals of pulsed flow. In 1 mM $CaCl_2$ solution, a pickup efficiency of <50% was achieved, whereas a 10 mM salt solution was sufficiently concentrated to preclude NP pickup. Catechol-Ca^{+2} complexation, confirmed independently by mass spectrometric characterization of products from aqueous solutions of 1,2-dihydroxybenzene and $CaCl_2$ [see fig. S9 and the study by Butler *et al.* (*37*)], effectively inhibits NP pickup and represents a means by which NP pickup efficiency could be controlled. In a similar fashion, the presence of Fe^{3+} in the solution during the experiment also led to a reduction (~50%) in pickup efficiency, as did the addition of free dopamine to the aqueous phase.

Fluorescence visualization

The known utility of fluorescent dyes (for example, alizarin, alizarin red S, and enhanced green fluorescent protein) (*38*, *39*) in estimating HA content in bones and HA-containing composite materials (*40*–*43*) led us to attempt to use these dyes to develop a fluorescence-based method for characterizing NP pickup. For example, alizarin powder was mixed with HA NPs in ethanol (1:10 weight ratio) for 2 hours, and the NPs were washed with ethanol three times and then suspended in ethanol at ~4.0 mg/ml. The alizarin-labeled HA NPs were visualized easily by fluorescence microscopy (Fig. 4) following spin coating onto a Si substrate. After NP pickup, the fluorescent signature was completely removed from the substrate, and a red fluorescence associated with polymer-decorated droplets was observed, indicative of incorporation of HA NPs onto the droplets.

Substrate effects—Toward "pickup and drop-off"

We attempted to establish the versatility of NP pickup using a variety of inorganic and plastic substrates including PDMS, mica, PET, and PEEK. For PDMS [surface oxidized by ultraviolet (UV)/ozone treatment] and mica, NP pickup proceeded successfully, with 70 to 80% efficiency, near to that found from the Si surfaces (figs. S10 and S11). However, we

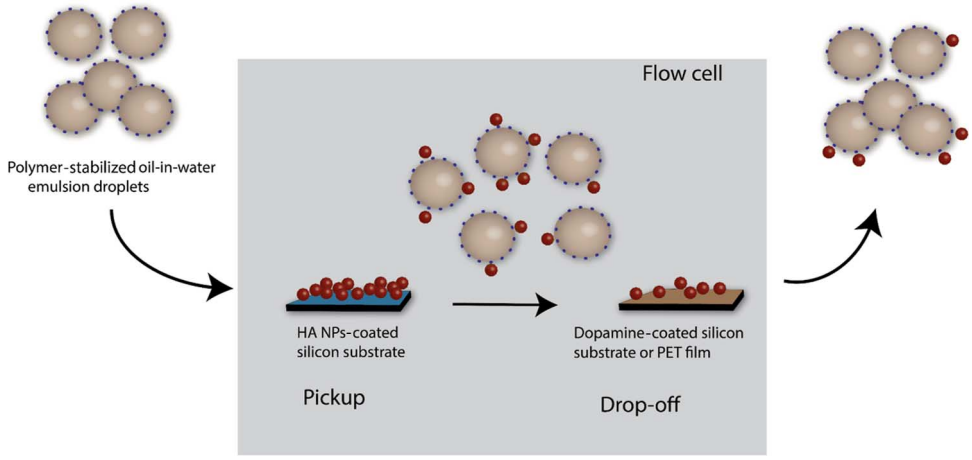

Fig. 5. Illustration of HA NP pickup and drop-off. The oil-in-water emulsion droplets stabilized by polymer **4** pick up HA NPs from the Si substrate and then drop them off downstream on the PDA-coated Si substrate or PET film.

observed essentially no NP pickup from plastic films composed of PET (fig. S12) and PEEK, suggesting a stronger interaction of the NPs with these substrates and/or a relative inability of the PC-polymer droplets to sufficiently wet these materials. We speculate that this results from the relative hydrophobicity of these plastics (PET and PEEK have water contact angle values of ~70°), but we do not have definitive evidence to support this. Nonetheless, this observation itself confirms that substrate composition may be exploited to adjust the relative extent of NP pickup or even provide an end-point destination for delivering NPs that are in transit via droplet carriers. From that standpoint, we then examined the potential of functional droplets to conduct pickup and drop-off in one "in-line" process, as illustrated in Fig. 5. Theoretical work by Balazs (*14*) showed that adjustment of NP-substrate interactions provides a means by which the concept may be realized. However, we are not aware of previous demonstrations of surface-to-surface NP transport or relocation, but we suggest that developing these methods would be exceptionally useful as a noninvasive technique for transferring NP properties (chemical, optical, magnetic, or electronic) from one material to another. Such a process is distinct from conventional cleaning or NP encapsulation and release processes and represents a potential route to efficient materials transport and/or recycling processes.

Our first attempt to drop off NPs subsequent to their initial pickup used a polydopamine (PDA)–modified substrate, intended to exploit the adhesive properties of PDA and its reported ability to promote NP deposition (*44*, *45*). PDA was applied to Si substrates by contact printing (*46*, *47*) to give smooth, light brown films (fig. S13B). The PDA-coated substrate was placed downstream from a HA NP–coated Si substrate, as shown in Fig. 5, using alizarin-labeled NPs for fluorescence tracking. Polymer **4**–stabilized droplets were used in over 300 pulsed flow intervals, and as seen in Fig. 6D, a fluorescent signature was transferred from the Si substrate to the PDA-coated substrate. Aside from the fluorescent signature, the substrate-to-substrate NP transfer was confirmed by SEM visualization of the HA particulates (insets of Fig. 6, B and D). By comparing the total area of fluorescent (red) regions on the PDA-coated substrate after NP deposition (Fig. 6D) to the NP pickup area (Fig. 6, A and C), an estimated 10 to 20% of the NPs were transferred to the PDA-coated substrate during the pickup and drop-off experiment. This represents an experimental realization of the pickup and drop-off concept proposed by Balazs (*14*), and future work will seek

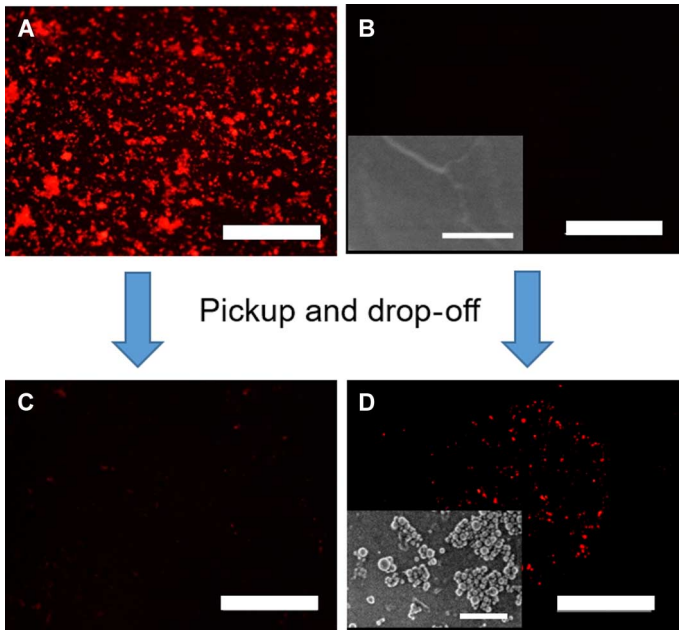

Fig. 6. HA NPs picked up by oil-in-water droplets stabilized by polymer 4 and dropped off on PDA-coated Si substrate. (**A**) Fluorescence micrograph of alizarin-labeled HA NP–coated substrates before pickup. (**B**) Fluorescence micrograph of PDA-coated Si substrate before drop-off and SEM image of PDA-coated Si substrate before drop-off (inset). (**C**) Fluorescence micrograph of alizarin-labeled HA NP–coated substrates after pickup. (**D**) Fluorescence micrograph of PDA-coated Si substrate after drop-off and SEM image of PDA-coated Si substrate after drop-off (inset). Scale bars, 500 μm for the micrographs and 500 nm for the SEM images [insets of (B) and (D)].

to exploit the process over a breadth of NP and substrate compositions. Notably, the PDA-coated Si substrate had an oily appearance under white light (fig. S13D), possibly due to rupture of some of the droplets on the surface. However, estimating qualitatively, the total number of droplets did not change over the course of the experiment. The inability of catechol-decorated droplets to pick up HA NPs from PET surfaces proved advantageous for pickup and drop-off

experiments: When the PDA-coated substrate was replaced with a PET film, a similar transfer of NPs from the Si substrate to PET was observed (fig. S14). Although these experiments are unoptimized with respect to efficiency, this nonetheless represents a key initial step to realizing the concept of NP relocation that may be advanced, by us and others, going forward.

CONCLUSION

We have demonstrated an effective approach to picking up HA NPs using oil-in-water emulsion droplets stabilized by PC-polyolefins with pendent catechol groups. Integration of catechol functionality into the PC-polyolefin surfactant provides an adhesive character to promote NP-droplet interactions and transport the NPs in a fluid-driven system. A measure of control over pickup efficiency was achieved by adjusting solution conditions (pH and salt concentration) and selection of substrate (from inorganic materials to plastics). Our attempts to deposit NPs on substrates following an initial pickup event led to an experimental realization of "pickup and drop-off," inspired by previous theoretical advances (*14*) and the cooperative action of particulate capture and deposition by live cells in vivo.

MATERIALS AND METHODS

Materials

HA NPs [$Ca_5(OH)(PO_4)_3$], white powder suspended in water, was purchased from Sigma-Aldrich. The original suspension was centrifuged and the supernatant was decanted. The resulting solid was then suspended in ethanol (4 mg/ml). 2,2,2-Trifluoroethanol (99+%) was purchased from Alfa Aesar. Polymer **6** with 25 mol % of phenyl ester–containing cyclooctene **5** was synthesized (M_n = 37.9 kDa; Đ = 1.90) in accordance with previously published procedure (*15*).

Synthesis of PC-polyolefins with catechol group

PC-substituted cyclooctene **1** (4.8 mmol, 1.40 g) and PFP-substituted cyclooctene **2** (3.2 mmol, 1.02 g) were dissolved in 4 ml of trifluoroethanol and degassed by three cycles of free-pump-thaw. In a separate vial, third-generation Grubbs catalyst was dissolved in 4 ml of degassed dichloromethane and rapidly injected into the monomer solution. Ethyl vinyl ether (0.5 ml) was added to terminate the polymerization after 1 hour. The reaction mixture was diluted with 2 ml of methanol and precipitated into acetone. Residual solvents were removed by placing the crude polymer under high vacuum overnight, affording 2.1 g of PC-PFPE polyolefins in 83% yield. GPC [1,1,1-trifluoroethanol (TFE) with 20 mM sodium trifluoroacetate, relative to poly(methyl methacrylate) (PMMA) standards]: M_n = 50.1 kDa, Đ = 1.90. The resulting polymer (1.1 g, 1.4 mmol PFPE, 40 mol % of PFPE, as determined by ^{1}H NMR spectroscopy) was redissolved in water (15 ml). Dopamine hydrochloride (1.57 mmol, 0.297 g) and triethylamine (1.57 mmol, 0.219 ml) were added. The reaction mixture was stirred for 10 hours and then transferred to a dialysis tubing with a molecular weight cutoff of 1 kDa to remove excess reagents and reaction by-products by dialyzing against methanol and water. Water was changed four to five times before lyophilization. Polymer was isolated as a grayish-brown solid in 50% yield. ^{1}H NMR (500 MHz, MeOD-d): 6.67 (br, 2H), 6.48 (br, 1H), 5.37 (br m, 4H), 4.20 (br, 3H), 3.58 (br, 2H), 3.31 (br, 4H), 3.15 (s, 9H), 2.7 (br, 1H), 2.59 (br 2H), 1.8 to 2.0 (br m, 8H), 1.2 to 1.7 (br m, 12H). GPC (TFE with 20 mM sodium trifluoroacetate, relative to PMMA standards): M_n = 70.6 kDa, Đ = 2.0. ^{1}H NMR shows 40 mol % of catechol groups.

Gel permeation chromatography

Molecular weight information was collected on an Agilent 1200 GPC instrument equipped with a degasser, a refractive index detector, a Polymer Standards Service (PSS) PFG guard column (8 mm × 50 mm), and three PSS-PFG analytical linear M columns (8 mm × 300 mm) using TFE with 20 mM sodium trifluoroacetate as mobile phase. The instrument was operated at 1 ml/min at 40°C and calibrated against PMMA standards. All samples were filtered through a 0.4-μm polytetrafluoroethylene filter before analysis.

Pendant drop tensiometry

A DataPhysics OCA-15 tensiometer was used in pendant drop mode to measure the interfacial tension between water and TCB using the PC-polyolefin with pendent catechol and phenyl groups, respectively. On the basis of the shape of the pendant drop, the interfacial tension between the liquids was calculated from the Young-Laplace equation using the instrument.

Preparation of alizarin-labeled HA NP

Alizarin (Sigma-Aldrich) was mixed with the HA NPs in ethanol at a 1:10 weight ratio. Then, the mixed suspension was agitated continuously using an orbital shaker at 300 rpm for 2 hours. The alizarin-labeled HA NPs were isolated from the suspension by centrifugation at 13,400 rpm for 15 min and then washed with ethanol.

Preparation of PDMS substrate

PDMS (Dow Corning Sylgard 184) substrates were prepared by mixing the base with the curing agent (10:1 by weight fraction) followed by degassing in a vacuum chamber for 30 min. The degassed mixture was poured into a rectangular mold with a depth of 1 mm and cured at 70°C for 4 hours. The PDMS samples were exposed to UV/ozone oxidation (Jelight 342) for 15 min to form an oxidized layer on the surface and used immediately.

PDA contact printing onto Si substrates

PDA was coated onto Si substrates by first immersing a solid PDMS stamp (2.0 cm × 1.0 cm × 0.2 cm) in a freshly prepared solution of dopamine hydrochloride (2 mg/ml) in tris-buffered solution (10 mM, pH 8.5) and agitated on the orbital shaker for 2 hours. Then the PDA-coated PDMS was rinsed three times in deionized water and dried by a gentle stream of nitrogen. This PDA-coated PDMS was pressed against a clean Si wafer with 100-g pressure on top for 20 min. PDA was then transferred to the Si surface after peeling the PDMS stamp off.

SUPPLEMENTARY MATERIALS

Supplementary material for this article is available at http://advances.sciencemag.org/cgi/content/full/2/10/e1601462/DC1

fig. S1. ^{13}C NMR spectra of polymers **3** and **4**.
fig. S2. ^{1}H NMR spectra of polymers **3** and **4**.
fig. S3. Oil-in-water emulsion droplets stabilized by polymer **4**.
fig. S4. Experimental setup for picking up HA NPs.
fig. S5. Control experiments using pH 7 water and droplets stabilized by polymer **6**.
fig. S6. HA NP–coated silicon substrate before and after pickup in 0.1 M NaOH solution.
fig. S7. HA NP–coated Si substrate before and after rinsing with pH 4 HCl solution.
fig. S8. Picking up HA NPs using polymer **4** in Ca^{2+}-rich solution.
fig. S9. Positive electrospray spectrum of an aqueous catechol/$CaCl_2$ (1:1 molar ratio) mixture in MeOH/water (1:1).
fig. S10. Picking up HA NPs from PDMS substrate.
fig. S11. Picking up HA NPs from mica.
fig. S12. Picking up HA NPs from PET film.
fig. S13. Optical micrographs of HA NPs picked up by oil-in-water droplets stabilized by polymer **4** and dropped off on PDA-coated Si substrate taken under white light.

fig. S14. HA NPs picked up by oil-in-water droplets stabilized by polymer **4** and dropped off on PET film.

REFERENCES AND NOTES

1. I. Mellman, Endocytosis and molecular sorting. *Annu. Rev. Cell Dev. Biol.* **12**, 575–625 (1996).
2. J. L. Goldstein, R. G. W. Anderson, M. S. Brown, Coated pits, coated vesicles, and receptor-mediated endocytosis. *Nature* **279**, 679–685 (1979).
3. S. Mukherjee, R. N. Ghosh, F. R. Maxfield, Endocytosis. *Physiol. Rev.* **77**, 759–803 (1997).
4. E. A. Meyer, R. K. Castellano, F. Diederich, Interactions with aromatic rings in chemical and biological recognition. *Angew. Chem. Int. Ed.* **42**, 1210–1250 (2003).
5. C. Chothia, J. Janin, Principles of protein–protein recognition. *Nature* **256**, 705–708 (1975).
6. J. E. Rothman, Mechanisms of intracellular protein transport. *Nature* **372**, 55–63 (1994).
7. T.-G. Iversen, T. Skotland, K. Sandvig, Endocytosis and intracellular transport of nanoparticles: Present knowledge and need for future studies. *Nano Today* **6**, 176–185 (2011).
8. U. Hersel, C. Dahmen, H. Kessler, RGD modified polymers: Biomaterials for stimulated cell adhesion and beyond. *Biomaterials* **24**, 4385–4415 (2003).
9. C.-K. Chan, D. A. Jans, Using nuclear targeting signals to enhance non-viral gene transfer. *Immunol. Cell Biol.* **80**, 119–130 (2002).
10. S. S. Parelkar, R. Letteri, D. Chan-Seng, O. Zolochevska, J. Ellis, M. Figueiredo, T. Emrick, Polymer–peptide delivery platforms: Effect of oligopeptide orientation on polymer-based DNA delivery. *Biomacromolecules* **15**, 1328–1336 (2014).
11. C. F. Nathan, H. W. Murray, Z. A. Cohn, The macrophage as an effector cell. *N. Engl. J. Med.* **303**, 622–626 (1980).
12. L. J. Raggatt, N. C. Partridge, Cellular and molecular mechanisms of bone remodeling. *J. Biol. Chem.* **285**, 25103–25108 (2010).
13. S. L. Teitelbaum, Bone resorption by osteoclasts. *Science* **289**, 1504–1508 (2000).
14. I. Salib, X. Yong, E. J. Crabb, N. M. Moellers, G. T. McFarlin IV, O. Kuksenok, A. C. Balazs, Harnessing fluid-driven vesicles to pick up and drop off Janus particles. *ACS Nano* **7**, 1224–1238 (2013).
15. I. Kosif, C. C. Chang, Y. Bai, A. E. Ribbe, A. C. Balazs, T. Emrick, Picking up nanoparticles with functional droplets. *Adv. Mater. Interfaces* **1**, 1400121 (2014).
16. K. Kratz, A. Narasimhan, R. Tangirala, S. Moon, R. Revanur, S. Kundu, H. S. Kim, A. J. Crosby, T. P. Russell, T. Emrick, G. Kolmakov, A. C. Balazs, Probing and repairing damaged surfaces with nanoparticle-containing microcapsules. *Nat. Nanotechnol.* **7**, 87–90 (2012).
17. Y. Bai, C.-C. Chang, X. Zhao, A. Ribbe, I. Bolukbasi, M. J. Szyndler, A. J. Crosby, T. Emrick, Mechanical restoration of damaged polymer films by "repair-and-go". *Adv. Funct. Mater.* **26**, 857–863 (2016).
18. I. A. Khalil, K. Kogure, H. Akita, H. Harashima, Uptake pathways and subsequent intracellular trafficking in nonviral gene delivery. *Pharmacol. Rev.* **58**, 32–45 (2006).
19. G. P. Robbins, R. L. Saunders, J. B. Haun, J. Rawson, M. J. Therien, D. A. Hammer, Tunable leuko-polymersomes that adhere specifically to inflammatory markers. *Langmuir* **26**, 14089–14096 (2010).
20. H. Jin, Y. Zheng, Y. Liu, H. Cheng, Y. Zhou, D. Yan, Reversible and large-scale cytomimetic vesicle aggregation: Light-responsive host–guest interactions. *Angew. Chem. Int. Ed.* **50**, 10352–10356 (2011).
21. H. Aoki, *Science and Medical Applications of Hydroxyapatite* (Ishiyaku Euroamerica, Kyoto, Japan, 1991).
22. W. Suchanek, M. Yoshimura, Processing and properties of hydroxyapatite-based biomaterials for use as hard tissue replacement implants. *J. Mater. Res.* **13**, 94–117 (1998).
23. H. Fleisch, R. Graham, G. Russell, M. D. Francis, Diphosphonates inhibit hydroxyapatite dissolution in vitro and bone resorption in tissue culture and in vivo. *Science* **165**, 1262–1264 (1969).
24. H. Zhou, J. Lee, Nanoscale hydroxyapatite particles for bone tissue engineering. *Acta Biomater.* **7**, 2769–2781 (2011).
25. L. Chen, J. M. Mccrate, J. C.-M. Lee, H. Li, The role of surface charge on the uptake and biocompatibility of hydroxyapatite nanoparticles with osteoblast cells. *Nanotechnology* **22**, 105708 (2011).
26. Y. Cai, Y. Liu, W. Yan, Q. Hu, J. Tao, M. Zhang, Z. Shi, R. Tang, Role of hydroxyapatite nanoparticle size in bone cell proliferation. *J. Mater. Chem.* **17**, 3780–3787 (2007).
27. S. P. Pathi, D. D. W. Lin, J. R. Dorvee, L. A. Estroff, C. Fischbach, Hydroxyapatite nanoparticle-containing scaffolds for the study of breast cancer bone metastasis. *Biomaterials* **32**, 5112–5122 (2011).
28. M. P. Ferraz, F. J. Monteiro, C. M. Manuel, Hydroxyapatite nanoparticles: A review of preparation methodologies. *J. Appl. Biomater. Biomech.* **2**, 74–80 (2004).
29. T. Kang, D. X. Oh, J. Heo, H.-K. Lee, S. Choy, C. J. Hawker, D. S. Hwang, Formation, removal, and reformation of surface coatings on various metal oxide surfaces inspired by mussel adhesives. *ACS Appl. Mater. Interfaces* **7**, 24656–24662 (2015).
30. J. M. W. Chan, J. P. K. Tan, A. C. Engler, X. Ke, S. Gao, C. Yang, H. Sardon, Y. Y. Yang, J. L. Hedrick, Organocatalytic anticancer drug loading of degradable polymeric mixed micelles via a biomimetic mechanism. *Macromolecules* **49**, 2013–2021 (2016).
31. L. He, D. E. Fullenkamp, J. G. Rivera, P. B. Messersmith, pH responsive self-healing hydrogels formed by boronate–catechol complexation. *Chem. Commun.* **47**, 7497–7499 (2011).
32. K. Kratz, K. Breitenkamp, R. Hule, D. Pochan, T. Emrick, PC-polyolefins: Synthesis and assembly behavior in water. *Macromolecules* **42**, 3227–3229 (2009).
33. T. Moriguchi, K. Yano, S. Nakagawa, F. Kaji, Elucidation of adsorption mechanism of bone-staining agent alizarin red S on hydroxyapatite by FT-IR microspectroscopy. *J. Colloid Interface Sci.* **260**, 19–25 (2003).
34. W. M. Chirdon, W. J. O'Brien, R. E. Robertson, Adsorption of catechol and comparative solutes on hydroxyapatite. *J. Biomed. Mater. Res. B Appl. Biomater.* **66B**, 532–538 (2003).
35. R. K. M. Khan, S. Torker, A. H. Hoveyda, Reactivity and selectivity differences between catecholate and catechothiolate Ru complexes. Implications regarding design of stereoselective olefin metathesis catalysts. *J. Am. Chem. Soc.* **136**, 14337–14340 (2014).
36. H. Lee, N. F. Scherer, P. B. Messersmith, Single-molecule mechanics of mussel adhesion. *Proc. Natl. Acad. Sci. U.S.A.* **103**, 12999–13003 (2006).
37. M. Butler, P. A. Mañez, G. M. Cabrera, P. Maître, Gas phase structure and reactivity of doubly charged microhydrated calcium (II)–catechol complexes probed by infrared spectroscopy. *J. Phys. Chem. A* **118**, 4942–4954 (2014).
38. S. Allegrini Jr., E. Rumpel, E. Kauschke, J. Fanghänel, B. König Jr., Hydroxyapatite grafting promotes new bone formation and osseointegration of smooth titanium implants. *Ann. Anat.* **188**, 143–151 (2006).
39. N. Kotobuki, K. Ioku, D. Kawagoe, H. Fujimori, S. Goto, H. Ohgushi, Observation of osteogenic differentiation cascade of living mesenchymal stem cells on transparent hydroxyapatite ceramics. *Biomaterials* **26**, 779–785 (2005).
40. P. Kasten, J. Vogel, R. Luginbühl, P. Niemeyer, M. Tonak, H. Lorenz, L. Helbig, S. Weiss, J. Fellenberg, A. Leo, H.-G. Simank, W. Richter, Ectopic bone formation associated with mesenchymal stem cells in a resorbable calcium deficient hydroxyapatite carrier. *Biomaterials* **26**, 5879–5889 (2005).
41. W. H. Harris, D. F. Travis, U. Friberg, E. Radin, The in vivo inhibition of bone formation by alizarin red S. *J. Bone Joint Surg. Am.* **46**, 493–508 (1964).
42. Y. Zhang, J. R. Venugopal, A. El-Turki, S. Ramakrishna, B. Su, C. T. Lim, Electrospun biomimetic nanocomposite nanofibers of hydroxyapatite/chitosan for bone tissue engineering. *Biomaterials* **29**, 4314–4322 (2008).
43. J. Venugopal, S. Low, A. T. Choon, T. S. Sampath Kumar, S. Ramakrishna, Mineralization of osteoblasts with electrospun collagen/hydroxyapatite nanofibers. *J. Mater. Sci. Mater. Med.* **19**, 2039–2046 (2008).
44. J. Ryu, S. H. Ku, H. Lee, C. B. Park, Mussel-inspired polydopamine coating as a universal route to hydroxyapatite crystallization. *Adv. Funct. Mater.* **20**, 2132–2139 (2010).
45. S. Saidin, P. Chevallier, M. R. Abdul Kadir, H. Hermawan, D. Mantovani, Polydopamine as an intermediate layer for silver and hydroxyapatite immobilisation on metallic biomaterials surface. *Mater. Sci. Eng. C* **33**, 4715–4724 (2013).
46. H.-W. Chien, W.-H. Kuo, M.-J. Wang, S.-W. Tsai, W.-B. Tsai, Tunable micropatterned substrates based on poly(dopamine) deposition via microcontact printing. *Langmuir* **28**, 5775–5782 (2012).
47. Q. Wei, B. Yu, X. Wang, F. Zhou, Stratified polymer brushes from microcontact printing of polydopamine initiator on polymer brush surfaces. *Macromol. Rapid Commun.* **35**, 1046–1054 (2014).

Acknowledgments: We thank R. Letteri for help with the pendant drop tensiometry. **Funding:** We acknowledge financial support for this work from the Department of Energy, Office of Basic Energy Sciences, Division of Materials Science and Engineering under award no. DE-SC0008876. **Author contributions:** Y.B., C.-C.C., I.B., and T.E. conceived and designed the study. Y.B. performed most of the experiments and imaging. C.-C.C. synthesized the copolymers. U.C. performed the electrospray ionization mass spectrometry measurement. Y.B., C.-C.C., A.J.C., and T.E. wrote the manuscript. All authors discussed the results and commented on the manuscript. **Competing interests:** The authors declare that they have no competing interests. **Data and materials availability:** All data needed to evaluate the conclusions in the paper are present in the paper and/or the Supplementary Materials. Additional data related to this paper may be requested from the authors.

Submitted 27 June 2016
Accepted 27 September 2016
Published 28 October 2016
10.1126/sciadv.1601462

Citation: Y. Bai, C.-C. Chang, U. Choudhary, I. Bolukbasi, A. J. Crosby, T. Emrick, Functional droplets that recognize, collect, and transport debris on surfaces. *Sci. Adv.* **2**, e1601462 (2016).

ScienceAdvances
AAAS

Functional droplets that recognize, collect, and transport debris on surfaces

Ying Bai, Chia-Chih Chang, Umesh Choudhary, Irem Bolukbasi, Alfred J. Crosby and Todd Emrick (October 28, 2016)

Sci Adv 2016, 2:.
doi: 10.1126/sciadv.1601462